FERTILITY

Dephosphorylation of protamine 2 at serine 56 is crucial for murine sperm maturation in vivo

Katsuhiko Itoh[1,2]*, Gen Kondoh[3], Hitoshi Miyachi[3], Manabu Sugai[4,5], Yoshiyuki Kaneko[1], Satsuki Kitano[3], Hitomi Watanabe[3], Ryota Maeda[6], Akihiro Imura[6], Yu Liu[1,7], Chizuru Ito[8], Shigeyoshi Itohara[9], Kiyotaka Toshimori[8,10], Jun Fujita[1,11]

The posttranslational modification of histones is crucial in spermatogenesis, as in other tissues; however, during spermiogenesis, histones are replaced with protamines, which are critical for the tight packaging of the DNA in sperm cells. Protamines are also posttranslationally modified by phosphorylation and dephosphorylation, which prompted our investigation of the underlying mechanisms and biological consequences of their regulation. On the basis of a screen that implicated the heat shock protein Hspa4l in spermatogenesis, we generated mice deficient in Hspa4l (*Hspa4l*-null mice), which showed male infertility and the malformation of sperm heads. These phenotypes are similar to those of *Ppp1cc*-deficient mice, and we found that the amount of a testis- and sperm-specific isoform of the Ppp1cc phosphatase (Ppp1cc2) in the chromatin-binding fraction was substantially less in *Hspa4l*-null spermatozoa than that in those of wild-type mice. We further showed that Ppp1cc2 was a substrate of the chaperones Hsc70 and Hsp70 and that Hspa4l enhanced the release of Ppp1cc2 from these complexes, enabling the freed Ppp1cc2 to localize to chromatin. Pull-down and in vitro phosphatase assays suggested the dephosphorylation of protamine 2 at serine 56 (Prm2 Ser^{56}) by Ppp1cc2. To confirm the biological importance of Prm2 Ser^{56} dephosphorylation, we mutated Ser^{56} to alanine in Prm2 (Prm2 S56A). Introduction of this mutation to *Hspa4l*-null mice (*Hspa4l*$^{-/-}$; *Prm2*$^{S56A/S56A}$) restored the malformation of sperm heads and the infertility of *Hspa4l*$^{-/-}$ mice. The dephosphorylation signal to eliminate phosphate was crucial, and these results unveiled the mechanism and biological relevance of the dephosphorylation of Prm2 for sperm maturation in vivo.

INTRODUCTION

Spermatogenesis is a stepwise process that requires coordination of mitosis, meiosis, and spermiogenesis, the process by which haploid spermatids mature into sperm (*1*, *2*). During the elongation phase of spermiogenesis, several critical processes occur to facilitate sperm motility, including nuclear compaction and chromatin condensation to generate the distinct head shape, as well as the redistribution of mitochondria within the flagella (*3*). Packaging haploid genomes is essential for nuclear condensation (*4*) and is achieved by replacing histones with transition proteins and, subsequently, with protamines, which are believed to be crucial in chromatin condensation, determination of sperm shape, and protection of the haploid genome (*5*).

A few species, including humans and mice, have two genes encoding protamines (Prms, P1/Prm1, and P2/Prm2), and the gene for Prm2, but not for Prm1, encodes a precursor protein, which undergoes proteolytic processing (*6*). It was reported more than 30 years ago that Prm2 is posttranslationally modified by phosphorylation and dephosphorylation in vivo (*7*); however, the underlying mechanism and biological consequences of this modification have not been clarified. Heat shock proteins (Hsps) are evolutionarily highly conserved, and they make up a group of structurally unrelated protein families (*8*). Hsps of 70 kDa (Hsp70s), such as Hsp70 (also termed Hspa1b) and Hsc70 (also termed Hspa8), are molecular chaperones involved in various protein-processing reactions, including protein transport across membranes (*9*). Hsp110 family members have a similar architecture to that of Hsp70s, except for the existence of a longer linker domain between the N-terminal adenosine triphosphatase domain and the C-terminal peptide-binding domain (*10*). These proteins act as nucleotide exchange factors (NEFs) (*11*, *12*) and accelerate the dissociation of nucleotides from Hsp70/adenosine diphosphate complexes and the subsequent release of Hsp70-bound substrates in an adenosine 5′-triphosphate (ATP)–dependent manner. Studies of the crystal structures of Hsp70 or Hsc70 in a complex with the NEF of Hsp110 have revealed how these chaperones cooperate in protein folding (*13*, *14*).

In a screen to identify proteins involved in spermatogenesis, we previously identified Hspa4l (also termed Apg-1) (*15*), which belongs to the Hsp110 family and is predominantly expressed in the testis (*16*). In the present study, we generated *Hspa4l* gene knockout mice to clarify the biological function of this Hsp110 member protein in vivo. Consistent with a previous report (*17*), we found that *Hspa4l*-deficient male mice were sterile and impaired in spermiogenesis. Furthermore, we found that the phosphatase Ppp1cc2 was a substrate of Hsp70s and that Hspa4l acted as a regulator of the binding of Hsp70s to Ppp1cc2, resulting in increased chromatin localization

[1]Department of Clinical Molecular Biology, Graduate School of Medicine, Kyoto University, Kyoto 606-8507, Japan. [2]Division of Medical Equipment Management, Department of Patient Safety, Kyoto University Hospital, Kyoto 606-8507, Japan. [3]Institute for Frontier Life and Medical Sciences, Kyoto University, Kyoto 606-8507, Japan. [4]Department of Molecular Genetics, Unit of Biochemistry and Bioinformative Sciences, Faculty of Medical Sciences, University of Fukui, 23-3 Matsuoka Shimoaizuki, Eiheiji-cho, Yoshida-gun, Fukui 910-1193, Japan. [5]Life Science Innovation Center, University of Fukui, 23-3 Matsuoka Shimoaizuki, Eiheiji-cho, Yoshida-gun, Fukui 910-1193, Japan. [6]Department of Hematology, Graduate School of Medicine, Kyoto University, Kyoto 606-8507, Japan. [7]Department of Molecular Gastroenterology and Hepatology, Graduate School of Medical Science, Kyoto Prefectural University of Medicine, Kyoto 602-8566, Japan. [8]Department of Functional Anatomy, Reproductive Biology and Medicine, Graduate School of Medicine, Chiba University, Chiba 260-8670, Japan. [9]Laboratory for Behavioral Genetics, RIKEN Brain Science Institute, Wako 351-0198, Japan. [10]Future Medical Research Center, Chiba University, Chiba 260-8670, Japan. [11]Department of Radiation Genetics, Graduate School of Medicine, Kyoto University, Kyoto 606-8501, Japan.
*Corresponding author. Email: katsu@virus.kyoto-u.ac.jp

of Ppp1cc2 and dephosphorylation of Prm2 in vivo.

RESULTS

Male mice deficient in *Hspa4l* are infertile and impaired in spermiogenesis

We generated *Hspa4l*-deficient mice by homologous recombination in E14 embryonic stem (ES) cells derived from the 129/Ola strain (fig. S1, A to D). The heterozygous and homozygous mice were viable, and intercrossing of heterozygous mice generated progeny at near Mendelian ratios ($Hspa4l^{+/+}$:$Hspa4l^{+/-}$:$Hspa4l^{-/-}$ = 25:55:31, n = 111). *Hspa4l*-null mice showed no gross abnormalities, but male mice were sterile after eight generations of backcrossing with C57BL/6 mice (Fig. 1A and fig. S2).

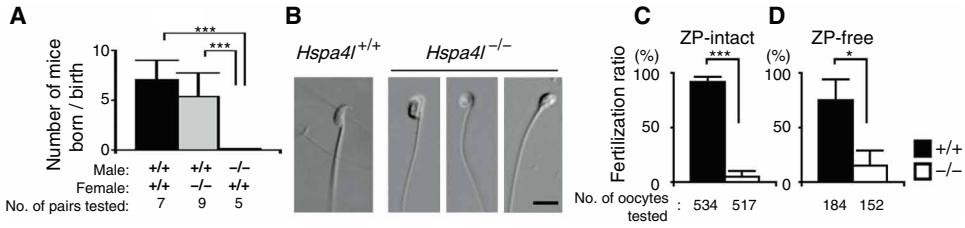

Fig. 1. Male mice deficient in *Hspa4l* are infertile, and their sperm heads show a rounded morphology. (**A**) Male mice of the indicated genotype ($Hspa4l^{+/+}$ or $Hspa4l^{-/-}$) were mated with the indicated female mice, and the resulting litter sizes was determined. Data are means ± SD. ***P < 0.001 by two-tailed Student's t test. (**B**) Representative images of the heads of sperm in the cauda epididymis of wild-type and *Hspa4l*-deficient mice. Scale bar, 10 μm. (**C** and **D**) Fertilization ratios with $Hspa4l^{-/-}$ sperm in vitro. We analyzed in vitro fertility using two male mice of each genotype with ZP-intact oocytes (C) or ZP-free oocytes (D) in five or three independent experiments, respectively. Data are means ± SD. *P < 0.05, ***P < 0.001 by two-tailed Student's t test.

Spermiogenesis was observed in the seminiferous tubules of $Hspa4l^{-/-}$ mice (fig. S3), and we found no abnormality in the number of spermatogonia or sperm of $Hspa4l^{-/-}$ mice (fig. S4). However, $Hspa4l^{-/-}$ spermatozoa in the cauda epididymidis had round heads (Fig. 1B). These spermatozoa could neither bind to zona pellucida (ZP)–intact oocytes (table S1) nor fertilize ZP-intact or ZP-free oocytes as efficiently as wild-type spermatozoa (Fig. 1C). Furthermore, these fertilized oocytes did not develop to the blastocyst stage (table S2).

To examine whether haploid cells in these mice contained a functional nucleus, we performed intracytoplasmic sperm injection (ICSI) and round spermatid injection (ROSI) assays. After ICSI, oocytes injected with $Hspa4l^{-/-}$ spermatozoa developed less efficiently than those injected with wild-type spermatozoa (table S3) and did not give rise to offspring (Table 1). After ROSI, in contrast, oocytes injected with $Hspa4l^{-/-}$ round spermatids developed comparably to those injected with wild-type spermatids (table S4) and efficiently gave rise to offspring (Table 2). Together, these results indicate that postmeiotic spermatids fail to differentiate into functional spermatozoa in $Hspa4l^{-/-}$ mice.

Table 1. Development of oocytes after intracytoplasmic injection of sperm. Results are from three independent experiments using two male mice of each genotype.

Genotype	No. of injected oocytes	No. of two-cell	No. of embryo transfer	No. of progeny
$Hspa4l^{+/+}$	49	40 (91.6%)*	40	12 (30.0%)**
$Hspa4l^{-/-}$	200	24 (12.0%)*	24	0 (0.0%)**

*$P = 1.10420691732578 \times 10^{-10}$. **$P$ = 0.0140905514994987 by Fisher's exact probability test.

Table 2. Development of oocytes injected with round spermatids. Results are from three independent experiments using two male mice of each genotype.

Genotype	No. of injected oocytes	No. of two-cell	No. of embryo transfer	No. of progeny
$Hspa4l^{+/+}$	166	71 (42.8%)*	63	16 (25.4%)**
$Hspa4l^{-/-}$	210	76 (36.2%)*	60	20 (33.3%)**

*P = 0.434569594957852. **P = 0.570464814844937 by Fisher's exact probability test.

Localization of Ppp1cc2 in a chromatin-binding fraction is impaired in *Hspa4l*-deficient mice

The phenotype of $Hspa4l^{-/-}$ mice is similar to that of *Ppp1cc* [protein phosphatase 1 gamma subunit (*Pp1γ*)]–deficient mice (*18*, *19*), and spermatozoa express a testis- and sperm-specific isoform of Ppp1cc (Ppp1cc2) (*20*, *21*). Because molecular chaperones can modulate protein localization (*9*), we examined whether the subcellular localization of Ppp1cc2 was altered in $Hspa4l^{-/-}$ spermatozoa. The distribution of Ppp1cc2 was comparable between $Hspa4l^{-/-}$ and wild-type sperm cells in cytoplasmic and nuclear fractions (fig. S5A). However, the amount of Ppp1cc2 localized in the chromatin-binding fraction was statistically significantly less in *Hspa4l*-null spermatozoa than that in wild types (Fig. 2, A and B, and fig. S5B). These results indicate that the subcellular localization of Ppp1cc2 is impaired in *Hspa4l*-deficient sperm.

To unveil an underlying mechanism, we tested whether Ppp1cc2 was a substrate of Hsp70s. An anti-Ppp1cc antibody co-immunoprecipitated Hsc70 (Fig. 2C), consistent with the protein phosphatase-1 (Pp1) interactome analysis of the human testis (*22*). It also co-precipitated Hsp70 (fig. S6). These results suggest that Ppp1cc could be a putative substrate of Hsp70s. Next, we tested whether Hspa4l acted as a co-chaperone for Hsp70s in sperm. An anti-Hspa4l antibody co-immunoprecipitated both Hsc70 (Fig. 2D) and Hsp70 (fig. S6B) from cauda epididymal sperm lysates. Together, these results suggest the formation of a chaperone-substrate complex between Hsp70s and Ppp1cc2, which includes Hspa4l as a co-chaperone. We postulated that the NEF activity of Hspa4l might accelerate the release of Ppp1cc2 from the complex, enabling the freed Ppp1cc2 to localize to chromatin. Consistent with this hypothesis, we co-immunoprecipitated Hsc70 with an anti-Ppp1cc antibody from the cytoplasmic and nuclear fractions of sperm cell lysates from wild-type mice, but not from the chromatin-binding fraction (fig. S7).

Ser^{56} of Prm2 is a putative target of the phosphatase Ppp1cc

A deficiency in Prm1 or Prm2 causes male infertility due to impaired sperm maturation (*23*), and Prms are posttranslationally modified

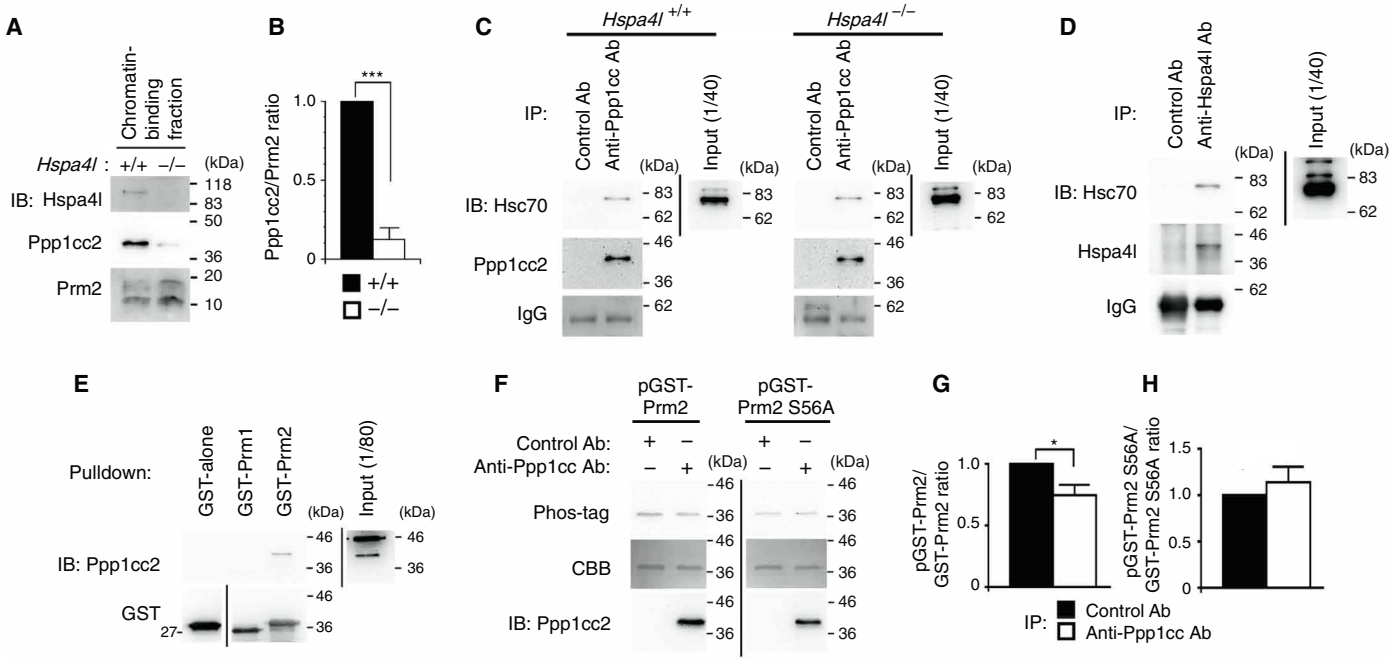

Fig. 2. Ppp1cc2 forms a chaperone-substrate complex with Hsc70, which includes Hspa4l, and Ppp1cc2 dephosphorylates the pSer^{56} of Prm2. (**A**) Chromatin-binding fractions from sperm of mice of the indicated genotypes were analyzed by Western blotting (IB) with antibodies (Abs) against the indicated proteins. Blots are representative of three experiments. (**B**) Ppp1cc2 to Prm2 ratios in the chromatin-binding fractions. Results indicate the relative Ppp1cc2:Prm2 ratio in *Hspa4l*-deficient sperm compared to that in wild-type sperm. Data are means ± SD of three independent experiments. ***P = 0.0003 by Welch's t test. (**C**) Interaction between Ppp1cc2 and Hsc70. Sperm cell lysates from the indicated mice were subjected to immunoprecipitation (IP) with control or anti-Ppp1cc antibodies and then analyzed by Western blotting with antibodies against the indicated proteins. Blots are representative of three experiments. IgG, immunoglobulin G. (**D**) Interaction between Hspa4l and Hsc70. Sperm cell lysates from the wild-type mice were subjected to immunoprecipitation with control or anti-Hspa4l antibodies and then analyzed by Western blotting with antibodies against the indicated proteins. Blots are representative of three experiments. (**E**) Interaction between Ppp1cc2 and Prm2. Sperm cell lysates from wild-type mice were subjected to GST pull-down experiments with the indicated fusion proteins. The samples were then analyzed by Western blotting with anti-GST antibody. Blots are representative of three experiments. (**F**) Ppp1cc2 dephosphorylates Ser^{56} of Prm2. Phosphatase assays were performed using the indicated fusion proteins as substrates. After the reactions were complete, phosphorylated or total substrates were detected by biotinylated Phos-tag or Coomassie blue staining (CBB), respectively. Data are representative of three experiments. (**G** and **H**) Results of three independent phosphatase assays using pGST-Prm2 (G) or pGST-Prm2 S56A (H). These substrates were dephosphorylated by samples immunoprecipitated by an anti-Ppp1cc antibody from the chromatin-binding fraction of epididymal sperm as described in Materials and Methods. Results indicate the relative ratios of phosphorylated proteins after the reaction using an anti-Ppp1cc antibody to those using a control antibody. Data are means ± SD. For (G), P = 0.0323; for (H), P = 0.2785 by Welch's t test.

(*5*, *24*). We examined whether Ppp1cc2 could bind to and modify Prms in chromatin. First, we performed a pull-down assay with recombinant Prm1 [glutathione *S*-transferase (GST)–Prm1] or the mature form of Prm2 (GST-Prm2). GST-Prm2, but not GST-Prm1, pulled down Ppp1cc2 from sperm cell lysates (Fig. 2E). Next, we substituted a putative phosphorylation site at Ser^{56} in GST-Prm2 with alanine (GST-Prm2 S56A) (*24*, *25*) and prepared phosphorylated GST-Prm2 or GST-Prm2 S56A (pGST-Prm2 or pGST-Prm2 S56A, respectively) using testicular cell lysate as a kinase. In phosphatase assays, we used these proteins as substrates, whereas for a source of phosphatase, proteins immunoprecipitated from the chromatin-binding fraction with an anti-Ppp1cc antibody or a control antibody were used. The former immunoprecipitate contained Ppp1cc2 (Fig. 2F) and dephosphorylated pGST-Prm2 but not pGST-Prm2 S56A (Fig. 2, G and H). Together, these data suggest that Ppp1cc2 can dephosphorylate Prm2 Ser^{56} in sperm chromatin.

Substitution of Prm2 Ser^{56} with alanine rescues the phenotype of *Hspa4l*$^{-/-}$ mice

To investigate the biological relevance of the dephosphorylation of Prm2-pSer^{56}, we generated *Prm2*$^{S56A/wt}$ and *Prm2*$^{S56D/wt}$ C57BL/6 mice, which harbored mutations of Ser^{56} to alanine or aspartate, respectively, by using the technology of CRISPR-Cas9 (*26*–*29*) (fig. S8, A and B). No mutations were identified in either strain in potential off-target sites (fig. S9, A and B), nor in neighboring sites of mutated regions (fig. S10). The ensuing heterozygous and homozygous mice were viable and showed no gross abnormalities. Similarly, both *Prm2*$^{S56A/S56A}$ and *Prm2*$^{S56D/S56D}$ male mice were fertile (fig. S8C), and their spermatozoa fertilized oocytes as efficiently as wild types in vitro (table S5 and table S6). These results suggest that these mutations were unlikely to affect the structural integrity of the nucleochromatin.

We intercrossed male *Prm2*$^{S56A/S56A}$ and *Prm2*$^{S56D/S56D}$ mice with *Hspa4l*$^{-/-}$ females. Although both *Hspa4l*$^{-/-}$ and *Hspa4l*$^{-/-}$; *Prm2*$^{S56D/S56D}$ male mice were infertile, the litter size from pairings with *Hspa4l*$^{-/-}$; *Prm2*$^{S56A/S56A}$ male mice was comparable to that with wild types and was statistically significantly greater than that with *Hspa4l*$^{-/-}$ or *Hspa4l*$^{-/-}$; *Prm2*$^{S56D/S56D}$ mice, indicating that the mutation of Prm2 Ser^{56} to an alanine (S56A), but not to a phosphomimetic of phosphoserine, aspartate (S56D), rescued the phenotype of infertility in *Hspa4l*-null mice (Fig. 3A). An in vitro fertilization experiment confirmed that *Hspa4l*$^{-/-}$; *Prm2*$^{S56A/S56A}$ spermatozoa could fertilize oocytes more efficiently than did *Hspa4l*$^{-/-}$ spermatozoa (Fig. 3B), and oocytes

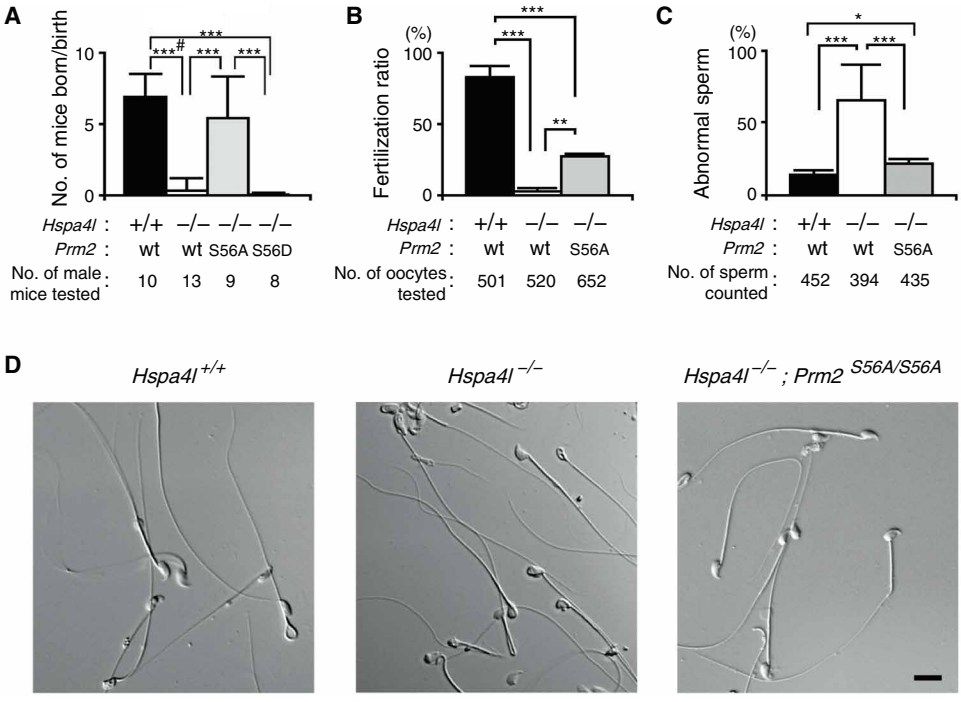

Fig. 3. Conversion of the codon encoding Ser^{56} to a codon encoding alanine in the *Prm2* locus rescues the infertile phenotype of *Hspa4l*$^{-/-}$ mice. (**A**) *Hspa4l*$^{-/-}$; *Prm2*$^{S56A/S56A}$ male mice are fertile. Male mice of the indicated genotypes were mated with wild-type (wt) female mice, and the resulting litter sizes were determined. Data are means ± SD. ***$P < 0.001$ by two-tailed Student's *t* test. "#" indicates Welch's *t* test. (**B**) Analysis of in vitro fertility. Two male mice of each the indicated genotypes were used. Data are means ± SD of three independent experiments. **$P < 0.01$, ***$P < 0.001$ by two-tailed Student's *t* test. (**C** and **D**) Substitution of Ser^{56} with alanine in Prm2 rescues the abnormal morphology of *Hspa4l*$^{-/-}$ sperm. (C) Results are from two male mice of each of the indicated genotypes. Data are means ± SD of three independent experiments. *$P < 0.05$, ***$P < 0.001$ by two-tailed Student's *t* test. (D) Representative images showing the morphology of the sperm from mice of the indicated genotypes. Scale bar, 10 μm.

these cells to the next generation (*23*). Prm1$^{+/-}$ and Prm2$^{-/-}$ male mice were also generated using TT2-XO ES cells (*31*) or by applying CRISPR-Cas9–mediated gene editing (*32*), respectively, and both sets of mice are infertile. Wu *et al.* (*33*) reported that the amount of Prm2 is reduced in step-15 spermatids of *Camk4* (Ca^{2+}/calmodulin-dependent protein kinase IV)–deficient mice, which are infertile on a mixed genetic background and that Prm2 is a putative substrate of Camk4. These studies showed the importance of protamines and their posttranslational regulation in mouse models. In humans, biochemical studies of male infertility demonstrated that changes in the protamine content of sperm chromatin, incomplete protamine P2 precursor processing, or alterations in the P1:P2 ratio contribute to male infertility (*34*, *35*).

Protamines have a series of small anchoring domains that contain positively charged amino acids (*35*), which bind to negatively charged DNA of the minor groove. In addition, protamines have an element containing serine and threonine residues, which are phosphorylated after synthesis. Phosphorylation may make protamines more negatively charged and decrease their affinity for negatively charged DNA. About 50 years ago, the serine residues of trout protamine were reported to be dephosphorylated after phosphorylation (*36*). More than 30 years ago, human Prm2 was reported to be posttranslationally modified by phosphorylation and dephosphorylation in vivo (*7*), and the Ser^{59} in human Prm2 can be phosphorylated (*25*). Furthermore, Ser^{56} in mouse Prm2, which is equivalent to Ser^{59} of human Prm2, is phosphorylated in vivo (*24*). However, it has not been clarified whether or how these sites are dephosphorylated.

fertilized with *Hspa4l*$^{-/-}$; *Prm2*$^{S56A/S56A}$ spermatozoa developed to the blastocyst stage in culture similarly to those fertilized with wild-type spermatozoa (table S7). Furthermore, morphological examination showed that the percentage of spermatozoa with a round head in *Hspa4l*$^{-/-}$; *Prm2*$^{S56A/S56A}$ mice was statistically significantly less than that in *Hspa4l*$^{-/-}$ mice (Fig. 3, C and D). Mitochondrial staining revealed that the mitochondria were localized to the round heads of spermatozoa from *Hspa4l*$^{-/-}$ mice. In contrast, the mitochondria in *Hspa4l*$^{-/-}$; *Prm2*$^{S56A/S56A}$ sperm localized in the mid-piece as did those in the sperm of wild-type mice (fig. S11). Together, these data suggest that the substitution of Ser^{56} with alanine rescued several aspects of the infertile phenotype and abnormal sperm morphology of *Hspa4l*$^{-/-}$ male mice. Furthermore, these results demonstrate that posttranslational modifications of Prms, in addition to those of histones (*5*), are biologically relevant and suggest that the dephosphorylation signal is a crucial biological process for murine sperm maturation in vivo.

DISCUSSION

Humans and mice have two genes that encode protamines (Prm1 and Prm2) (*30*). Previous reports demonstrated that chimeric male mice generated by injecting Prm1$^{+/-}$ or Prm2$^{+/-}$ ES cells into C57BL/6 blastocysts transmit neither the mutant nor the wild-type allele from

Although the importance of pSer^{56} dephosphorylation was supported by experiments in which this residue was substituted with an alanine, the results of experiments in which Ser^{56} was substituted with an aspartate, a phosphomimetic of phospho-serine, raise the question of why *Prm2*$^{S56D/S56D}$ male mice are fertile (fig. S8C and table S6). Multisite phosphorylation of human Prm2 has been reported (*37*). Many regulatory proteins are regulated by multisite phosphorylation, and some of them have proved to be multisite-phosphorylated by sequential intramolecular phosphorylation cascade, suggesting a complex posttranslational network including kinases and phosphatases (*38*, *39*). For example, the hepatitis C virus nonstructural protein 5A (NS5A) is first phosphorylated at Ser^{232}, and this phosphorylation primes the sequential phosphorylation of other serine residues of NS5A, which are important for viral replication (*40*, *41*). On the basis of these reports and our observations of the mutant mice in this study, we postulate that phosphorylation of Prm2 at Ser^{56} might prime a sequential intramolecular phosphorylation cascade. Ppp1cc2 might also dephosphorylate other serine residues of Prm2, and this step

could be crucial for sperm maturation. Consistent with this postulation, *Prm2*$^{S56A/S56A}$ or *Hspa4l*$^{-/-}$; *Prm2*$^{S56A/S56A}$ male mice were fertile (Fig. 3, A and B, and tables S5 and S7), because substitution of Ser^{56} with alanine would be expected to block the phosphorylation cascade. On the other hand, substitution of Ser^{56} with aspartate would not block this cascade. We suggest that because Ppp1cc2 could dephosphorylate the other phosphorylated serine residues primed by the aspartate substitution, *Prm2*$^{S56D/S56D}$ male mice were fertile (fig. S8C and table S7). However, *Hspa4l*$^{-/-}$; *Prm2*$^{S56D/S56D}$ male mice were infertile because of the impaired recruitment of Ppp1cc (Fig. 3A and table S8). Our current study has just began to unravel the sperm maturation network by kinases and phosphatases, and detailed mechanisms remain to be clarified in experiments with Ppp1cc-null mice or with antibodies that recognize specific phosphorylated serine residues.

Pp1 is a major protein serine and threonine phosphatase and consists of a catalytic and a regulatory subunit (*42*). Although several isoforms exist that are involved in a wide range of cellular processes, the catalytic subunits are encoded by only three genes (*Ppp1ca*, *Ppp1cb*, and *Ppp1cc*) (*43*). Two groups have reported that *Ppp1cc*-deficient male mice are infertile without apparent abnormality in other tissues (*18*, *19*). To unveil the underlying mechanisms, potential targets or interacting molecules of Ppp1cc2 were examined in the testis and sperm (*21*, *22*, *44*–*46*). Here, we demonstrated that Hsc70 and Hsp70 regulated the localization of Ppp1cc2 to the chromatin-binding fraction, together with Hspa4l, and that Ppp1cc2 could dephosphorylate Prm2 at Ser^{56} in chromatin. The biological relevance of this dephosphorylation signal was confirmed by generating *Hspa4l*$^{-/-}$; *Prm2*$^{S56A/S56A}$ mice.

Several limitations of this study need to be addressed. Regulatory subunits of Pp1 are thought to control its localization, activity, and substrate specificity (*47*). The identity of the Ppp1cc2-specific regulatory subunit in the chromatin-binding fraction of sperm remains to be clarified. Next, because of technical limitations, we could not show the phosphorylation state of Prm2 at Ser^{56} in *Hspa4l*-null mice directly. Such an experiment would provide additional and clear evidence that the dephosphorylation of Prm2 at Ser^{56} is crucial for sperm maturation.

Although genetic analysis of human *Prm2* has been widely performed, pathogenic mutations are estimated to be rare in infertile patients (*48*). On the other hand, a report showed that the amount of Hspa4l in the sperm of patients with asthenozoospermia or teratospermia is less than that in the sperm of healthy controls (*49*). Because the posttranslational regulatory mechanism of Prm2 proposed in this study potentially associates with male infertility in humans, it would be worth examining the phosphorylation state of Ser^{59} of human Prm2 in the sperm of infertile patients, as well as investigating any alterations of *Hspa4l* or *Ppp1cc*.

MATERIALS AND METHODS

Antibodies

Polyclonal antibodies against Hspa4l (Apg-1, N-96), Hsp70 (K-20), Hsc70 (K-19), protamine 1 (M-51), protamine 2 (N-20), Ppp1cc (Pp1γ C-19), acrosin (C-14), and GST (Z-5), as well as anti-mouse Hsc70 (B-6) and anti–α-tubulin (B-7) monoclonal antibodies were purchased from Santa Cruz Biotechnology. Phycoerythrin-conjugated anti–α6-integrin (G0H3) and anti-EpCAM (G8.8) monoclonal antibodies were from BD Pharmingen. Anti-mouse Hsp70 and Hsc70 (B-6) antibodies were biotinylated, whereas Alexa Fluor 647 or fluorescein isothiocyanate was conjugated to anti-mouse CD117 (c-Kit, ACK2) or anti-rat IgG κ (K4F5, Coulter), respectively. Horseradish peroxidase (HRP)–conjugated anti-rabbit, anti-mouse, and anti-goat IgG polyclonal antibodies, as well as HRP-conjugated streptavidin were from DakoCytomation.

Plasmids and preparation of recombinant proteins

To prepare pX330-Prm2, we designed a *Prm2* gene–specific guide RNA sequence using the CRISPR design tool (http://crispr.mit.edu/) (*50*), and ligated annealed oligonucleotides of 5′-CACCGacaggcgctgctctcgtaag-3′ and 5′-AAACcttacgagagcagcgcctgtC-3′ into the Bbs I site of pX330-U6-Chimeric_BB-CBh-hSpCas9 (*26*). We amplified fragments containing the coding sequence of Prm1 and the mature form of Prm2 by reverse transcription polymerase chain reaction (PCR), which were ligated into pGEX-4 T-1 (GE Healthcare Japan) to construct pGEX/Prm1 and pGEX/Prm2, respectively. To generate pGEX/Prm2/S56A, we mutated the cloned sequence of the mature form of Prm2 to substitute Ser^{56} with alanine using the QuikChange site-directed mutagenesis kit (Stratagene) and ligated the fragment into pGEX-4 T-1. BL21 cells transformed with pGEX/Prm1, pGEX/Prm2, or pGEX/Prm2/S56A were lysed, and the recombinant proteins GST-Prm1, GST-Prm2, and GST-Prm2 S56A were prepared using a glutathione sepharose column (GE Healthcare Japan), respectively.

Generation of *Hspa4l*-deficient and *Prm2* mutant mice

We constructed the *Hspa4l*-targeting vector, which was designed to replace a 0.4-kb genomic fragment containing its promoter and the first exon with a neomycin resistance gene cassette (fig. S1A). We generated *Hspa4l*-deficient mice by homologous recombination in E14 ES cells derived from the mouse strain 129/Ola. After targeting, we microinjected ES clones into C57BL/6 blastocysts and mated chimeric mice with C57BL/6 mice to obtain F_1 *Hspa4l*$^{+/-}$ mice. The mutant mice were backcrossed to C57BL/6 mice for at least eight generations before being used in experiments, unless otherwise indicated in the figure legends. To genotype the mice, we performed PCR analysis using extracted genomic DNAs from tails and the following sets of primers (a and b in fig. S1A): for the targeted locus, 5′-ctgctaaagcgcatgctccaga-3′ and 5′-cttagaagagcgtccgcgagaca-3′; and for the wild-type locus, 5′-ctgccctagattttccgatagagagt-3′ and 5′-gctacagcgatgtagcagttgag-3′. We generated *Prm2*$^{S56A/wt}$ and *Prm2*$^{S56D/wt}$ mice using a CRISPR-Cas9–mediated genome-editing strategy, with minor modification as described by Mashiko *et al.* (*26*–*29*) (fig. S8, A and B). We injected a circular plasmid, pX330-Prm2 (5 ng/μl), and single-stranded oligonucleotides (10 ng/μl; for *Prm2*$^{S56A/wt}$, 5′-cacacaggggccaccaccaccacagacacaggcgctgcGcCAgGaagaggctacataggatccacaagag gcgtcggtcatgc-3′; and for *Prm2*$^{S56D/wt}$: 5′-caggggccaccaccaccacagacacaggcgctgcGACcgtaagaggctacataggatccacaagaggcgtcgg-3′) into the pronuclei of fertilized oocytes of the C57BL/6 strain and transferred two-cell stage embryos into the oviducts of pseudopregnant ICR females. Genomic DNAs of offspring were extracted and analyzed by PCR using the following sets of primers: for the mutated locus of *Prm2*$^{S56A/wt}$, 5′-agacacaggcgctgcGcCAgG-3′ and 5′-ggaaggcagcagggtttagatgg-3′; for the wild-type locus of *Prm2*$^{S56A/wt}$, 5′-agacacaggcgctgctctcgt-3′ and 5′-ggaaggcagcagggtttagatgg-3′; for the mutated locus of *Prm2*$^{S56D/wt}$, 5′-cacagacacaggcgctgcGAC-3′ and 5′-ggaaggcagcagggtttagatgg-3′; and for wild-type locus of *Prm2* $^{S56D/wt}$, 5′-cacagacacaggcgctgctct-3′ and 5′-ggaaggcagcagggtttagatgg -3′. To confirm the mutations, we amplified genomic fragments by PCR using a set of primers, 5′-gggcctggacaagaccatgaac-3′ and 5′-cttggctccaggcagaatccac-3′, and sequenced directly using a sequence primer, 5′-ggaaggcagcaggtttagatgg-3′. Potential off-target sites (OT-1 to OT-7) were found

at the website CRISPR Design (http://crispr.mit.edu/) (*50*), and genomic fragments containing the off-target sequences were amplified and sequenced using the primers listed in table S9. All animal experiments were reviewed and approved by the Animal Committee of Kyoto University.

Preparation of subcellular fractions

Cauda epididymides were homogenized on ice with a glass Teflon homogenizer in buffer-150 [150 mM NaCl, 50 mM tris (pH 7.4), leupeptin (2 μg/ml), and 1 mM phenylmethylsulfonyl fluoride (PMSF)], passed through nylon mesh (40 μm), and incubated for 60 min at 4°C after adding Triton X-100 (to a final concentration of 1.0%). After centrifugation at 5000*g* for 5 min, the supernatant was analyzed as the nucleocytoplasmic fraction. The pellet was extracted with 2 M NaCl for 20 min at 4°C and centrifuged, and the supernatant was designated as the NaCl fraction. The remaining pellet was digested with deoxyribonuclease I for 20 min at 37°C and centrifuged and was used as the chromatin-binding fraction. In some experiments, homogenized cauda epididymides were passed through nylon mesh, solubilized in buffer-150 containing 0.5% Nonidet P40, and analyzed as the cytoplasmic fraction. The pellet was further solubilized in buffer containing 1.0% Triton X-100 and analyzed as the nuclear fraction.

Immunoprecipitation, GST pull-down assay, and Western blotting

For co-immunoprecipitation of Hspa4l or Ppp1cc, we prepared sperm lysates in buffer-150 containing 1.0% Triton X-100 or 0.5% Nonidet P40, immunoprecipitated with anti-Hspa4l or anti-Ppp1cc antibodies, respectively, and analyzed the samples by Western blotting using the antibodies indicated in the figure legends. For the GST pull-down assay, we incubated GST-Prm1 or GST-Prm2 in sperm cell lysates prepared in buffer-150 containing 0.5% Nonidet P40, pulled down protein complexes with glutathione sepharose beads, and subjected the immunoprecipitates to Western blotting analysis using an anti-Ppp1cc antibody. For detection of basic proteins, we used Bjerrum and Schafer-Nielsen buffer [48 mM tris (pH 9.2), 39 mM glycine, 20% methanol, and 0.01% SDS] as the transfer buffer. After Western blotting, in some experiments, band densities were quantitatively measured with Image Lab software (Bio-Rad).

In vitro phosphatase assay

We lysed dissociated testicular cells in kination buffer [150 mM NaCl, 10 mM tris (pH 7.5), 10 mM $MgCl_2$, 0.5 mM dithiothreitol (DTT), leupeptin (2 μg/ml), 1 mM PMSF, 1 mM $NaVO_4$, and 1 mM NaF] containing 1.0% Triton X-100, and phosphorylated GST-Prm2 or GST-Prm2 S56A using the lysates as a kinase in the presence of 2 mM ATP at 30°C for 45 min. After kination, phosphorylated GST-fusion proteins were prepared using a glutathione sepharose column, suspended in phosphatase buffer (10 mM Hepes, 1 mM $MnCl_2$, and 1 mM DTT) and used as substrates. For the phosphatase, we used proteins precipitated by an anti-Ppp1cc antibody from the chromatin-binding fraction of epididymal sperm and incubated the substrates in phosphatase buffer at 30°C for 45 min. After the reaction, the products were subjected to SDS–polyacrylamide gel electrophoresis, and phosphorylated or total products were analyzed by chemiluminescence using biotinylated Phos-tag (Phos-tag biotin BTL-104, Manac Inc.) or Coomassie blue staining, respectively. Densities of products were quantitatively measured using Image Lab software.

Preparation of dissociated testicular cells and flow cytometric analysis of spermatogenic cells

We prepared dissociated testicular cells by a two-step enzymatic digestion using collagenase and trypsin and performed flow cytometric analysis of spermatogonia as described previously (*51*, *52*). To analyze the DNA content of cells, dissociated testicular cells were fixed with methanol, stained with propidium iodide, and analyzed on an Epics XL flow cytometer (Coulter).

In vitro fertilization and sperm-egg binding assays

We performed an in vitro fertilization assay and a sperm-egg binding assay as described previously (*53*). In some experiments, we used ZP-free oocytes prepared as described previously (*54*).

ICSI and ROSI

We performed ICSI according to a previously described procedure (*55*). ROSI was performed according to a previously described procedure (*56*) with modification. Briefly, we prepared dissociated testicular cells and injected round spermatids into superovulated oocytes with a piezo-actuated micromanipulator. Oocytes that received round spermatids were placed in Ca^{2+}-free CZB medium containing 10 mM $SrCl_2$ for 20 min after the injection and then were cultured for 1 hour for their activation. We incubated oocytes that successfully received ICSI or ROSI in CZB medium and transferred them to the oviducts of pseudopregnant ICR females after reaching the two-cell stage unless indicated otherwise in the figure legends.

Sperm count

Sperm were collected from the vas deferens, and the number of sperm was counted using a hemocytometer.

Sperm morphology

Sperm from cauda epididymides were incubated in HTF medium for 1 hour, and their morphology was observed by microscopy. Sperm were also stained with Hoechst33342 (5 μg/ml) and 50 nM Mito Tracker Green FM (Invitrogen) in HTF medium at 37°C for 30 min and then were analyzed using a fluorescence microscope, BZ-9000 (Keyence, Japan). Signals of Hoechst33342 or Mito Tracker Green FM were visualized as blue or green, respectively, and images were merged using software provided with the BZ-9000 microscope.

Fertility tests

We placed male mice with females for about 2 months to observe whether pregnancy ensured, confirming copulation by checking for vaginal plugs every morning and recording the numbers of litters produced.

Histological and immunocytochemical analyses

Testes were fixed with paraformaldehyde and embedded in paraffin. Mounted sections were deparaffinized, rehydrated, stained with hematoxylin and labeled antibodies, and analyzed using fluorescence microscopy for immunohistochemical analysis. For toluidine blue staining, testes were fixed with osmium and embedded in Epon.

Data analysis

Statistical analyses were performed using the JMP statistical software package (SAS Institute Inc.). Differences between the means of two groups were analyzed for statistical significance using two-tailed Student's *t* tests or Welch's *t* test when Levene's test rejected

homoscedasticity (cutoff, 0.05). Two nominal variables were analyzed using Fisher's exact probability test. A value of $P < 0.05$ was considered to be statistically significant for all analyses.

SUPPLEMENTARY MATERIALS

www.sciencesignaling.org/cgi/content/full/12/574/eaao7232/DC1
Fig. S1. Generation of *Hspa4l*$^{-/-}$ mice.
Fig. S2. *Hspa4l*$^{-/-}$ male mice of a mixed strain are not sterile.
Fig. S3. Histological analysis of testes.
Fig. S4. The numbers of spermatogonia and sperm are normal in *Hspa4l*$^{-/-}$ mice.
Fig. S5. Subcellular localization of Ppp1cc2.
Fig. S6. Ppp1cc2 forms a chaperone-substrate complex with Hsp70.
Fig. S7. Subcellular analysis of the interaction of Ppp1cc2 with Hsc70.
Fig. S8. Generation of *Prm2*$^{S56A/wt}$ and *Prm2*$^{S56D/wt}$ mice and demonstration that *Prm2*$^{S56A/S56A}$ and *Prm2*$^{S56D/S56D}$ male mice are fertile.
Fig. S9. No mutations in potential off-target sites.
Fig. S10. No mutations in neighboring sites of mutated regions.
Fig. S11. Morphological analysis of sperm.
Table S1. Sperm binding assays.
Table S2. Development of oocytes in culture after fertilization with sperm from *Hspa4l*$^{-/-}$ mice.
Table S3. Development of oocytes in culture after intracytoplasmic injection of sperm.
Table S4. Development of oocytes in culture after injection with round spermatids.
Table S5. Development of oocytes in culture after fertilization with sperm from *Prm2*$^{S56A/S56A}$ mice.
Table S6. Development of oocytes in culture after fertilization with sperm from *Prm2*$^{S56D/S56D}$ mice.
Table S7. Development of oocytes in culture after fertilization with sperm from *Hspa4l*$^{-/-}$; *Prm2*$^{S56A/S56A}$ mice.
Table S8. Development of oocytes in culture after fertilization with sperm from *Hspa4l*$^{-/-}$; *Prm2*$^{S56D/S56D}$ mice.
Table S9. Primers used for sequencing potential off-target sites.

REFERENCES AND NOTES

1. D. G. de Rooij, L. D. Russell, All you wanted to know about spermatogonia but were afraid to ask. *J. Androl.* **21**, 776–798 (2000).
2. S. Z. Jan, G. Hamer, S. Repping, D. G. de Rooij, A. M. M. van Pelt, T. L. Vormer, Molecular control of rodent spermatogenesis. *Biochim. Biophys. Acta* **1822**, 1838–1850 (2012).
3. L. O'Donnell, Mechanisms of spermiogenesis and spermiation and how they are disturbed. *Spermatogenesis* **4**, e979623 (2015).
4. D. Miller, M. Brinkworth, D. Iles, Paternal DNA packaging in spermatozoa: More than the sum of its parts? DNA, histones, protamines and epigenetics. *Reproduction* **139**, 287–301 (2010).
5. J. Bao, M. T. Bedford, Epigenetic regulation of the histone-to-protamine transition during spermiogenesis. *Reproduction* **151**, R55–R70 (2016).
6. D. Carré-Eusébe, F. Lederer, K. H. D. Lê, S. M. Elsevier, Processing of the precursor of protamine P2 in mouse. Peptide mapping andN-terminal sequence analysis of intermediates. *Biochem. J.* **277**, 39–45 (1991).
7. F. H. Pruslin, E. Imesch, R. Winston, T. C. Rodman, Phosphorylation state of protamines 1 and 2 in human spermatids and spermatozoa. *Gamete Res.* **18**, 179–190 (1987).
8. K. Richter, M. Haslbeck, J. Buchner, The heat shock response: Life on the verge of death. *Mol. Cell* **40**, 253–266 (2010).
9. M. P. Mayer, B. Bukau, Hsp70 chaperones: Cellular functions and molecular mechanism. *Cell. Mol. Life Sci.* **62**, 670–684 (2005).
10. L. Shaner, K. A. Morano, All in the family: Atypical Hsp70 chaperones are conserved modulators of Hsp70 activity. *Cell Stress Chaperones* **12**, 1–8 (2007).
11. Z. Dragovic, S. A. Broadley, Y. Shomura, A. Bracher, F. U. Hartl, Molecular chaperones of the Hsp110 family act as nucleotide exchange factors of Hsp70s. *EMBO J.* **25**, 2519–2528 (2006).
12. H. Raviol, H. Sadlish, F. Rodriguez, M. P. Mayer, B. Bukau, Chaperone network in the yeast cytosol: Hsp110 is revealed as an Hsp70 nucleotide exchange factor. *EMBO J.* **25**, 2510–2518 (2006).
13. J. P. Schuermann, J. Jiang, J. Cuellar, O. Llorca, L. Wang, L. E. Gimenez, S. Jin, A. B. Taylor, B. Demeler, K. A. Morano, P. J. Hart, J. M. Valpuesta, E. M. Lafer, R. Sousa, Structure of the Hsp110:Hsc70 nucleotide exchange machine. *Mol. Cell* **31**, 232–243 (2008).
14. S. Polier, Z. Dragovic, F. U. Hartl, A. Bracher, Structural basis for the cooperation of Hsp70 and Hsp110 chaperones in protein folding. *Cell* **133**, 1068–1079 (2008).
15. Y. Kaneko, H. Nishiyama, K. Nonoguchi, H. Higashitsuji, M. Kishishita, J. Fujita, A novel *hsp110*-related gene, *apg-1*, that is abundantly expressed in the testis responds to a low temperature heat shock rather than the traditional elevated temperatures. *J. Biol. Chem.* **272**, 2640–2645 (1997).
16. Y. Kaneko, T. Kimura, H. Nishiyama, Y. Noda, J. Fujita, Developmentally regulated expression of APG-1, a member of heat shock protein 110 family in murine male germ cells. *Biochem. Biophys. Res. Commun.* **233**, 113–116 (1997).
17. T. Held, I. Paprotta, J. Khulan, B. Hemmerlein, L. Binder, S. Wolf, S. Schubert, A. Meinhardt, W. Engel, I. M. Adham, Hspa4l-deficient mice display increased incidence of male infertility and hydronephrosis development. *Mol. Cell. Biol.* **26**, 8099–8108 (2006).
18. S. Varmuza, A. Jurisicova, K. Okano, J. Hudson, K. Boekelheide, E. B. Shipp, Spermiogenesis is impaired in mice bearing a targeted mutation in the protein phosphatase 1cgamma gene. *Dev. Biol.* **205**, 98–110 (1999).
19. N. Sinha, P. Puri, A. C. Nairn, S. Vijayaraghavan, Selective ablation of Ppp1cc gene in testicular germ cells causes oligo-teratozoospermia and infertility in mice. *Biol. Reprod.* **89**, 128 (2013).
20. Y. Kitagawa, K. Sasaki, H. Shima, M. Shibuya, T. Sugimura, M. Nagao, Protein phosphatases possibly involved in rat spermatogenesis. *Biochem. Biophys. Res. Commun.* **171**, 230–235 (1990).
21. J. V. Silva, M. J. Freitas, M. Fardilha, Phosphoprotein phosphatase 1 complexes in spermatogenesis. *Curr. Mol. Pharmacol.* **7**, 136–146 (2014).
22. M. Fardilha, S. L. C. Esteves, L. Korrodi-Gregório, A. P. Vintém, S. C. Domingues, S. Rebelo, N. Morrice, P. T. W. Cohen, O. A. B. da Cruz e Silva, E. F. da Cruz e Silva, Identification of the human testis protein phosphatase 1 interactome. *Biochem. Pharmacol.* **82**, 1403–1415 (2011).
23. C. Cho, W. D. Willis, E. H. Goulding, H. Jung-Ha, Y. C. Choi, N. B. Hecht, E. M. Eddy, Haploinsufficiency of protamine-1 or -2 causes infertility in mice. *Nat. Genet.* **28**, 82–86 (2001).
24. A. M. Brunner, P. Nanni, I. M. Mansuy, Epigenetic marking of sperm by post-translational modification of histones and protamines. *Epigenetics Chromatin* **7**, 2 (2014).
25. F. Chirat, A. Arkhis, A. Martinage, M. Jaquinod, P. Chevaillier, P. Sautière, Phosphorylation of human sperm protamines HP1 and HP2: Identification of phosphorylation sites. *Biochim. Biophys. Acta* **1203**, 109–114 (1993).
26. L. Cong, F. A. Ran, D. Cox, S. Lin, R. Barretto, N. Habib, P. D. Hsu, X. Wu, W. Jiang, L. A. Marraffini, F. Zhang, Multiplex genome engineering using CRISPR/Cas systems. *Science* **339**, 819–823 (2013).
27. P. Mali, L. Yang, K. M. Esvelt, J. Aach, M. Guell, J. E. DiCarlo, J. E. Norville, G. M. Church, RNA-guided human genome engineering via Cas9. *Science* **339**, 823–826 (2013).
28. H. Wang, H. Yang, C. S. Shivalila, M. M. Dawlaty, A. W. Cheng, F. Zhang, R. Jaenisch, One-step generation of mice carrying mutations in multiple genes by CRISPR/Cas-mediated genome engineering. *Cell* **153**, 910–918 (2013).
29. D. Mashiko, Y. Fujihara, Y. Satouh, H. Miyata, A. Isotani, M. Ikawa, Generation of mutant mice by pronuclear injection of circular plasmid expressing Cas9 and single guided RNA. *Sci. Rep.* **3**, 3355 (2013).
30. R. Balhorn, The protamine family of sperm nuclear proteins. *Genome Biol.* **8**, 227 (2007).
31. N. Takeda, K. Yoshinaga, K. Furushima, K. Takamune, Z. Li, S.-i. Abe, S.-i. Aizawa, K.-i. Yamamura, Viable offspring obtained from Prm1-deficient sperm in mice. *Sci. Rep.* **6**, 27409 (2016).
32. S. Schneider, M. Balbach, J. F. Jikeli, D. Fietz, D. Nettersheim, S. Jostes, R. Schmidt, M. Kressin, M. Bergmann, D. Wachten, K. Steger, H. Schorle, Re-visiting the Protamine-2 locus: Deletion, but not haploinsufficiency, renders male mice infertile. *Sci. Rep.* **6**, 36764 (2016).
33. J. Y. Wu, T. J. Ribar, D. E. Cummings, K. A. Burton, G. S. McKnight, A. R. Means, Spermiogenesis and exchange of basic nuclear proteins are impaired in male germ cells lacking Camk4. *Nat. Genet.* **25**, 448–452 (2000).
34. R. Oliva, Protamines and male infertility. *Hum. Reprod. Update* **12**, 417–435 (2006).
35. R. Balhorn, A model for the structure of chromatin in mammalian sperm. *J. Cell Biol.* **93**, 298–305 (1982).
36. C. J. Ingles, G. H. Dixon, Phosphorylation of protamine during spermatogenesis in trout testis. *Proc. Natl. Acad. Sci. U.S.A.* **58**, 1011–1018 (1967).
37. A. Pirhonen, A. innala-Kankkunen, P. H. Mënpää, P2 protamines are phosphorylated in vitro by protein kinase C, whereas P1 protamines prefer cAMP-dependent protein kinase. A comparative study of five mammalian species. *Eur. J. Biochem.* **223**, 165–169 (1994).
38. C. Dai, W. Gu, p53 post-translational modification: Deregulated in tumorigenesis. *Trends Mol. Med.* **16**, 528–536 (2010).
39. S. M. Rubin, Deciphering the retinoblastoma protein phosphorylation code. *Trends Biochem. Sci.* **38**, 12–19 (2013).
40. S.-C. Hsu, C.-W. Lo, T.-C. Pan, K.-Y. Lee, M.-J. Yu, Serine 235 is the primary NS5A hyperphosphorylation site responsible for hepatitis C virus replication. *J. Virol.* **91**, e00194-17 (2017).
41. S.-C. Hsu, C.-N. Tsai, K.-Y. Lee, T.-C. Pan, C.-W. Lo, M.-J. Yu, Sequential S232/S235/S238 Phosphorylation of the Hepatitis C Virus Nonstructural Protein 5A. *J. Virol.* **92**, 01295-18 (2018).
42. Y. Shi, Serine/threonine phosphatases: Mechanism through structure. *Cell* **139**, 468–484 (2009).
43. G. B. G. Moorhead, L. Trinkle-Mulcahy, A. Ulke-Lemée, Emerging roles of nuclear protein phosphatases. *Nat. Rev. Mol. Cell Biol.* **8**, 234–244 (2007).

44. H. Henderson, G. Macleod, C. Hrabchak, S. Varmuza, New candidate targets of protein phosphatase-1c-gamma-2 in mouse testis revealed by a differential phosphoproteome analysis. *Int. J. Androl.* **34**, 339–351 (2011).
45. E. Heroes, B. Lesage, J. Görnemann, M. Beullens, L. Van Meervelt, M. Bollen, The PP1 binding code: A molecular-lego strategy that governs specificity. *FEBS J.* **280**, 584–595 (2013).
46. J. V. Silva, S. Yoon, P.-J. de Bock, A. V. Goltsev, K. Gevaert, J. F. F. Mendes, M. Fardilha, Construction and analysis of a human testis/sperm-enriched interaction network: Unraveling the PPP1CC2 interactome. *Biochim. Biophys. Acta* **1861**, 375–385 (2017).
47. M. Bollen, W. Peti, M. J. Ragusa, M. Beullens, The extended PP1 toolkit: Designed to create specificity. *Trends Biochem. Sci.* **35**, 450–458 (2010).
48. V. W. Aoki, G. L. Christensen, J. F. Atkins, D. T. Carrell, Identification of novel polymorphisms in the nuclear protein genes and their relationship with human sperm protamine deficiency and severe male infertility. *Fertil. Steril.* **86**, 1416–1422 (2006).
49. X. X. Liu, X. F. Shen, F.-J. Liu, Screening targeted testis-specific genes for molecular assessment of aberrant sperm quality. *Mol. Med. Rep.* **14**, 1594–1600 (2016).
50. P. D. Hsu, D. A. Scott, J. A. Weinstein, F. A. Ran, S. Konermann, V. Agarwala, Y. Li, E. J. Fine, X. Wu, O. Shalem, T. J. Cradick, L. A. Marraffini, G. Bao, F. Zhang, DNA targeting specificity of RNA-guided Cas9 nucleases. *Nat. Biotechnol.* **31**, 827–832 (2013).
51. K. Takubo, M. Ohmura, M. Azuma, G. Nagamatsu, W. Yamada, F. Arai, A. Hirao, T. Suda, Stem cell defects in ATM-deficient undifferentiated spermatogonia through DNA damage-induced cell-cycle arrest. *Cell Stem Cell* **2**, 170–182 (2008).
52. T. Masuda, K. Itoh, H. Higashitsuji, H. Higashitsuji, N. Nakazawa, T. Sakurai, Y. Liu, H. Tokuchi, T. Fujita, Y. Zhao, H. Nishiyama, T. Tanaka, M. Fukumoto, M. Ikawa, M. Okabe, J. Fujita, Cold-inducible RNA-binding protein (Cirp) interacts with Dyrk1b/Mirk and promotes proliferation of immature male germ cells in mice. *Proc. Natl. Acad. Sci. U.S.A.* **109**, 10885–10890 (2012).
53. E. Deguchi, T. Tani, H. Watanabe, S. Yamada, G. Kondoh, Dipeptidase-inactivated tACE action in vivo: Selective inhibition of sperm-zona pellucida binding in the mouse. *Biol. Reprod.* **77**, 794–802 (2007).
54. G. L. Nicolson, R. Yanagimachi, H. Yanagimachi, Ultrastructural localization of lectin-binding sites on the zonae pellucidae and plasma membranes of mammalian eggs. *J. Cell Biol.* **66**, 263–274 (1975).
55. Y. Kimura, R. Yanagimachi, Intracytoplasmic sperm injection in the mouse. *Biol. Reprod.* **52**, 709–720 (1995).
56. H. Miki, J. Lee, K. Inoue, N. Ogonuki, Y. Noguchi, K. Mochida, T. Kohda, H. Nagashima, F. Ishino, A. Ogura, Microinsemination with first-wave round spermatids from immature male mice. *J. Reprod. Dev.* **50**, 131–137 (2004).

Acknowledgments: We thank C. Stocking-Harbers and A. Tanaka for critical reading of the manuscript and preparation of figures, respectively. The plasmid pX330-U6-Chmeric_BB-CBh-hSpCas9 was obtained from Addgene (Addgene plasmid 42230). **Funding:** This work was supported, in part, by the Smoking Research Foundation of Japan and Grants-in-Aid for Scientific Research (KAKENHI, 16H01387) from the Japan Society for the Promotion of Science.
Author contributions: K.I. and J.F. designed research; K.I., G.K., H.W., R.M., A.I., and Y.L. performed cellular or biochemical research; C.I. and K.T. performed histochemical analysis; H.M., Y.K., S.K., and S.I. generated mutant mice; K.I., G.K., H.M., M.S., and J.F. analyzed and interpreted the data; K.I. performed the statistical analysis; G.K., M.S., S.I., C.I., and K.T. made comments; K.I. wrote the manuscript; and G.K., M.S., C.I., and J.F. edited the manuscript.
Competing interests: The authors declare that they have no competing interests. **Data and materials availability:** All data needed to evaluate the conclusions in the paper are present in the paper or the Supplementary Materials. The gene-manipulated mouse lines *Prm2*$^{S56A/S56A}$, *Prm2*$^{S56D/S56D}$, and *Hspa4l*$^{-/-}$ were deposited into the Riken BioResource Center or Center for Animal Resources and Development, Kumamoto University, with stock numbers RBRC09931, RBRC09932, and 2379, respectively.

Submitted 19 August 2017
Accepted 12 March 2019
Published 26 March 2019
10.1126/scisignal.aao7232

Citation: K. Itoh, G. Kondoh, H. Miyachi, M. Sugai, Y. Kaneko, S. Kitano, H. Watanabe, R. Maeda, A. Imura, Y. Liu, C. Ito, S. Itohara, K. Toshimori, J. Fujita, Dephosphorylation of protamine 2 at serine 56 is crucial for murine sperm maturation in vivo. *Sci. Signal.* **12**, eaao7232 (2019).

Science Signaling

Dephosphorylation of protamine 2 at serine 56 is crucial for murine sperm maturation in vivo

Katsuhiko Itoh, Gen Kondoh, Hitoshi Miyachi, Manabu Sugai, Yoshiyuki Kaneko, Satsuki Kitano, Hitomi Watanabe, Ryota Maeda, Akihiro Imura, Yu Liu, Chizuru Ito, Shigeyoshi Itohara, Kiyotaka Toshimori and Jun Fujita

Sci. Signal. **12** (574), eaao7232.
DOI: 10.1126/scisignal.aao7232

Protamine dephosphorylation for fertility

During the final stage of spermatogenesis, protamines tightly package DNA in the mature sperm. Itoh *et al*. generated mice deficient in the heat shock protein and chaperone Hspa4l, which is implicated in spermatogenesis. The mice were infertile with malformed sperm heads, a phenotype similar to that of mice deficient in the phosphatase Ppp1cc2. The authors showed that Hspa4l was required to release Ppp1cc2 from a complex with other chaperones, enabling its translocation to chromatin. In vitro studies showed that Ppp1cc2 dephosphorylated protamine 2 at Ser^{56}. Expression of the unphosphorylatable protamine 2 S56A mutant reversed the infertility of Hspa4l-deficient mice, suggesting that the dephosphorylation of protamine 2 at Ser^{56} is important for its role in sperm maturation.

Science Signaling (ISSN 1937-9145) is published by the American Association for the Advancement of Science, 1200 New York Avenue NW, Washington, DC 20005. The title *Science Signaling* is a registered trademark of AAAS.